Modeling and Control of the Engine Turbine for the Purpose of the Electricity Generation

LUCJAN SETLAK, RAFAŁ KOWALIK
Department of Avionics and Control Systems
Polish Air Force University
ul. Dywizjonu 303 nr 35, 08-521 Deblin
POLAND
l.setlak@law.mil.pl, r.kowalik@law.mil.pl, http://www.law.mil.pl/index.php/pl/

Abstract - In the combined propulsion system of an aircraft, one of the main elements responsible for the process of generating electric energy is an electric machine connected to the propulsion system, the rotor and the blades. The article presents technical problems related to the use of motorized sources of electric energy for servicing civil and military flying aircraft. The main purpose of the article was to model the process of propulsion turbine control in the field of electricity generation. A mathematical model of air flow through the turbine of an aircraft engine was presented. The process of generating electricity using an asynchronous motor was discussed. In the final part of this work, based on a critical analysis of the literature on the subject of research, created model of the propulsion system based on the use of a mathematical apparatus and simulation tests evaluating the work of an asynchronous machine, practical conclusions were formulated.

Key-Words: - Modeling and Control Process, Turbine of the Drive Unit, Simulations, Electricity Generation

1 Introduction

Modern aircraft engines contain more and more electrical components, which is to ensure greater efficiency and safety. Asynchronous machines thanks to their relatively simple construction and operation as well as ease of repair and maintenance, guaranteeing long and reliable operation, are the most common electromechanical transducers and are widely used in systems with different dynamic structures. They are the most commonly used source of machine drive in industry, and their universality and the variety of applications contributes to a better understanding of their properties and dynamic processes taking place [1], [2].

Asynchronous electric motors, often a source of mechanical energy in propulsion systems, dynamically affect the drive gear transmission. For this reason, it is reasonable to take into account in mathematical models of propulsion systems description of dynamic phenomena that occur in the engine [3], [4], [5].

1.1 Types of generators used

1.1.1 DC generator

The DC generator is made of a stator - a fixed part and a rotor - a movable part. The electric current is generated because the rotor rotates in a magnetic field created by a permanent magnet or by an external constant current source of the stator winding. Power stations with this type of generator are called low speed, because the rotational speed is about 40 rpm.

Moreover, no gear is used, so the propeller shaft from the rotor is directly connected with armature in generator [6], [7], [8]. The characteristics of the generated current is then, like the air flow, non-linear and non-uniform, because the amount of electricity generated is closely related to the air flow speed at a given time. Therefore, it is necessary to use a voltage regulator to standardize the resulting current. If it is necessary to obtain alternating current, an inverter is also used (Fig. 1).

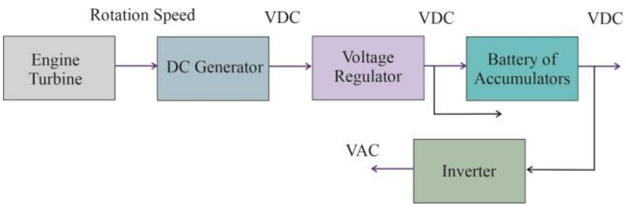

Fig. 1 Example scheme for using a DC generator

1.1.2 AC generator

AC generators are based on the phenomenon of SEM electromotive force induction due to conductor movement in the magnetic field of electromagnetic induction. Asynchronous generators can operate with variable or constant spin speed, but practically except for wind energy they are not used. They are highly reliable, durable and relatively cheap, which is a key factor in electricity production. The

phenomenon of slipping in them is extremely desirable because the generator slightly changes its speed in the event of a change in drive torque. An additional advantage is the possibility of increasing the slip by increasing the rotor resistance. This reduces the susceptibility to transmission failures and less wear. It is important to power the stator windings before starting work to magnetize it. Usually an external device is needed, e.g. capacitors or a battery, because it is undesirable to draw energy from the network [9], [10], [11].
Asynchronous generators are machines where the use of constant rotational speed prevents the optimal use of air flow energy. Bipolar generators partially solve this problem. In weak winds they can work at a lower speed. There is also a solution in the form of building two separate generators in one nacelle for different air speeds [12], [13].

2 Model of the Propulsion System

The turbine propulsion system, in terms of mechanical parts, consists mainly of the blade adjustment mechanism, hub with blades, or relatively long drive shafts, generator and gears. The presented model represents inertial systems related to the turbine and generator. The torque from the turbine wheel together with the blade adjustment mechanism is the largest component of all moments, since its percentage is about 90%, while the torque from the generator is about 10% of the total torque. Moreover, the generator represents the highest torsional stiffness at the same time [14], [15].
A relatively common and acceptable way of modeling the propulsion system for analyzing the operation of the power system is to introduce the assumption that in such a system there are only two uniform rotational masses; the generator with the gearbox represents the first mass, and the rotor with the hub the second mass [16]. This type of arrangement is shown in the figure below (Fig. 2).

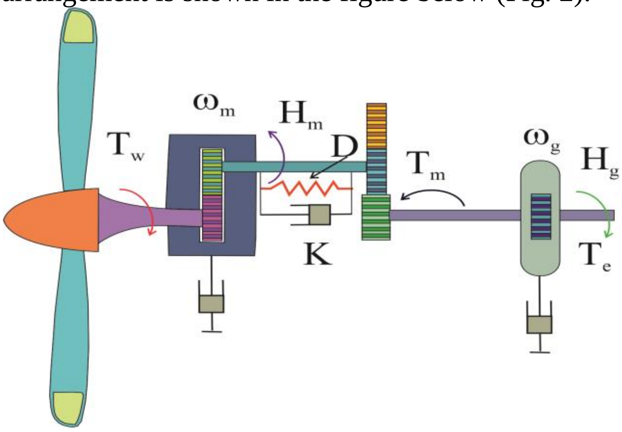

Fig. 2 Propulsion system moments distribution [16]

where:
n - gear ratio, ω_g, ω_m - generator and rotor angular velocity, H_g, H_m - generator and rotor inertia constant, K - system stiffness constant, D - system damping constant, T_w - torque provided by air, T_e - torque generated from the generator.
Based on the above drawing, the motion equation for the generator is described by the following formula (1):

$$H_g \frac{d\omega_g}{dt} = T_e + \frac{T_m}{n} \tag{1}$$

Considering that the turbine has a propeller shaft connected to the generator via a transmission, rigid transmission system should not be considered [17], [18], [19].
It is necessary to introduce an additional equation that will allow to show the relationship between the turbine wheel and the generator rotor, which can be written using the following equation (2).

$$H_m \frac{d\omega_m}{dt} = T_w - T_m \tag{2}$$

The resulting torque T_m can be represented in the form (3) and (4):

$$T_m = K\frac{\theta}{n} + D\frac{\omega_g - \omega_m}{n} \tag{3}$$

$$\omega_g - \omega_m = \frac{d\theta}{dt} \tag{4}$$

where: θ - is the angle between the rotor of the aircraft engine and the rotor of the generator.

3 Modeling of an Asynchronous Generator

The driving force from the air turbine rotor is converted into electricity through an AC or DC generator. The alternator can be both synchronous and asynchronous.
This generator has a three-phase generator rotor winding (A_R, B_R, C_R) and stator (A_s, B_s, C_s) in which it rotates. The diagram is presented in the next figure (Fig. 3). Supplying the stator windings with three-phase current during the rotation of the rotor creates a rotating electromagnetic field [20], [21], [22].
In the case where the rotor rotates synchronously to the rotation of the magnetic field in the stator or the magnetic field, the rotational speed of the rotating

field is called the synchronous speed ω_s. When the armature rotation is higher than the magnetic field rotation, then alternating current is induced to the target network or receiver. If this speed is lower than the synchronous speed, then the generator works as a motor that requires power.

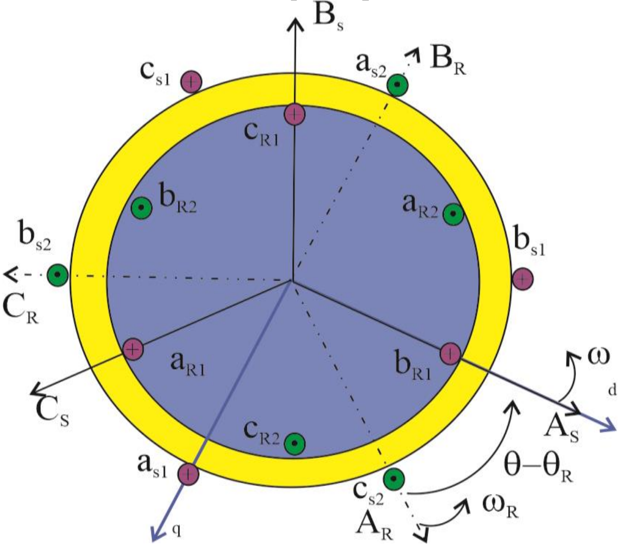

Fig. 3 Diagram of the asynchronous generator windings [16]

In order to analyze the power system, the mathematical model of the asynchronous generator in question assumes [23], [24], [25]:

– the current flow in the stator is correct when directed to the electricity grid,
– stator and rotor windings are arranged sinusoidally along the air gaps in such a way that they correspond to the turbine rotor,
– stator and rotor windings are symmetrical,
– the electric capacity of the windings is negligible,
– magnetic hysteresis and saturation of induction are negligible,
– the air compartments in the stator do not have the desired effect on the induction (passive resistance of induction) of the rotor relative to its location,
– the air compartments in the rotor do not have the desired effect on the inductor (inductive passive resistance) of the stator relative to its position.

It should be noted that further refining the modeling assumptions increases the difficulty in obtaining the correct data.

3.1 *0dq* reference system

The set of equations of the asynchronous generator model is usually converted into a bound model with any reference system in which the machine is transformed into the so-called *0dq* reference system model [26], [27], [28].

The axis *dq* representing the induction of a generator is used in the simulation as the basic variable of flux coupling. It based on a two-axis performances of the fifth order. Mathematical transformations are used in the analysis and simulation of three-phase systems, mainly to separate variables, in order to facilitate solving difficult equations with coefficients that change over time. *Park's* transformation separates and changes the stator variables into the *dq* reference system. The positive axis *d* of this system is consistent with the magnetic axis of the field winding, and the positive axis *q* is in accordance with the direction of rotation or shifts the positive axis *d* by $\pi/2$. The axes *ds* and *qs* correspond to the axes of the stator and quadrature, while *dr* and *qr* correspond to the axes of the rotor and its quadrature [29], [30].

3.2 Asynchronous generator model

The parameters of electric generators are often presented as a reference to a base value or a reference value. This allows for a significant simplification of calculations, regardless of the amount of current. The diagram is presented below in the form (5):

$$walue = \frac{current\ value\ (quantity)}{base\ value\ or\ reference\ value\ (the\ same\ quantity)} \quad (5)$$

These models, although very complicated, are often described in many books or articles [31], [32], [33]. The two main models can be specified from them.

The first full model includes the electromagnetic waveforms of the stator and rotor, which contain four variables of electromagnetic state. This model is also known as the fifth order model.

The second, simplified model omits the stator waveforms, containing two variables of electromagnetic state. In the literature, this model may be called the third order model because it takes into account two state variables and the speed of the generator. The two main models are discussed below [34], [35], [36].

In the fifth order model, equations related to the stator current voltage axis V_{ds} and quadrature axis of the stator current voltage V_{qs} are needed associated with amperage along the axis I_{ds} and I_{qs}.

The complete model is expressed in the *0dq* reference system rotating at synchronous speed, obtaining positive current, and is represented by the formulas (6) - (9):

– for magnetic streams:

$$\varphi_{ds} = X_s I_{ds} + X_m I_{dr} \quad (6)$$

$$\varphi_{qs} = X_s I_{qs} + X_m I_{qr} \quad (7)$$

$$\varphi_{dr} = X_r I_{dr} + X_m I_{ds} \quad (8)$$

$$\varphi_{qr} = X_r I_{qr} + X_m I_{qs} \quad (9)$$

– for currents:

$$V_{dr} = -R_s I_{ds} + \omega_s \varphi_{qs} - \frac{d\varphi_{ds}}{dt} \quad (10)$$

$$V_{qs} = -R_s I_{qs} - \omega_s \varphi_{ds} - \frac{d\varphi_{qs}}{dt} \quad (11)$$

$$0 = -R_r I_{dr} + s\omega_s \varphi_{qr} - \frac{d\varphi_{dr}}{dt} \quad (12)$$

$$0 = -R_r I_{qr} - s\omega_s \varphi_{dr} - \frac{d\varphi_{qr}}{dt} \quad (13)$$

where: indexes *s* and *r* - mean respectively the stator and rotor quantities, and indexes *d* and *q* refer to the axes *d* and *q* in the reference frame rotating with synchronous speed, φ - represents magnetic flux, *V* - voltage and *I* - current.
In the case of a traditional induction machine, the rotor voltage V_{dr} and V_{qr} are equal to zero, because the current is applied only to the stator. The variables ω_s and ω_g are synchronous speed and generator rotor, respectively. Parameters R_s, X_s, X_m, R_r and X_r - mean respectively the stator resistance, its reactance, mutual reactance as well as the rotor resistance and its reactance [37], [38], [39].
Rotor slip *s* is a positive factor during propulsion but a negative factor during power generation, which is defined by formula (14):

$$s = \frac{\omega_s - \omega_g}{\omega_s} \quad (14)$$

The electric torque produced is (15):

$$T_e = \varphi_{qr} I_{dr} - \varphi_{dr} I_{qr} \quad (15)$$

This moment is positive when it drives the system, and negative when it generates current.
Ultimately, active and reactive power is determined by the formulas (16) and (17):

$$P_{aktywna} = V_{ds} I_{ds} + V_{qs} I_{qs} \quad (16)$$

$$Q_{bierna} = V_{qs} I_{ds} - V_{ds} I_{qs} \quad (17)$$

Total power is the sum of active and reactive power, resulting in (18):

$$P = V_{ds} I_{ds} + V_{qs} I_{qs} + V_{qs} I_{ds} - V_{ds} I_{qs} \quad (18)$$

The third-order model assumes simplification by omitting transient stator states, which will reduce the fifth-order generator model. This is a commonly used method when presenting simulation of stability [40], [41], [42], [43].
This is done by omitting factors $\frac{d\varphi_{ds}}{dt}$ and $\frac{d\varphi_{qs}}{dt}$ in equations (10) - (11), which is equivalent to the assumption of infinitely fast electromagnetic waveforms in the stator windings.
The transformed model takes the following form, described by equations (19) - (32).

$$\varphi_{ds} = X_s I_{ds} + X_m I_{dr} \quad (19)$$

$$\varphi_{qs} = X_s I_{qs} + X_m I_{qr} \quad (20)$$

$$\varphi_{dr} = X_r I_{dr} + X_m I_{ds} \quad (21)$$

$$\varphi_{qr} = X_r I_{qr} + X_m I_{qs} \quad (22)$$

$$V_{dr} = -R_s I_{ds} + \omega_s \varphi_{qs} \quad (23)$$

$$V_{qs} = -R_s I_{qs} - \omega_s \varphi_{ds} \quad (24)$$

$$0 = -R_r I_{dr} + s\omega_s \varphi_{qr} - \frac{d\varphi_{dr}}{dt} \quad (25)$$

$$0 = -R_r I_{qr} - s\omega_s \varphi_{dr} - \frac{d\varphi_{qr}}{dt} \quad (26)$$

$$s = \frac{\omega_s - \omega_g}{\omega_s} \quad (27)$$

$$T_e = \varphi_{qr} I_{dr} - \varphi_{dr} I_{qr} \quad (28)$$

$$P_{aktywna} = V_{ds} I_{ds} + V_{qs} I_{qs} \quad (29)$$

$$Q_{bierna} = V_{qs} I_{ds} - V_{ds} I_{qs} \quad (30)$$

$$P = V_{ds} I_{ds} + V_{qs} I_{qs} + V_{qs} I_{ds} - V_{ds} I_{qs} \quad (31)$$

$$P_{AIR} = \frac{1}{2} \rho A V^3 \quad (32)$$

4 Work Control Systems

4.1 Power control

From formula (32) it follows that air velocity has the greatest impact on the power produced, because it is raised to the third power. A two-fold increase in air speed results in an eightfold increase in power. Given this relationship, it is necessary to design a system that will prevent sudden high changes in energy produced, so as not to damage both the generator and the elements of the power grid to which the turbine is connected. Such a system should ensure operational safety and control over the output power much greater than that used for power supply [44], [45], [46].

The air velocity range that allows to achieve the highest efficiency is 10 to 15 m/s. Above this speed, the turbine control system will have to prevent the turbine rotational speed from adversely increasing in such a way that the rotor is then driven by a smaller force, and that the load on the structure of the entire electrical network of the aircraft is smaller. To achieve this, various methods of controlling aerodynamic forces are used, which results in control of the power obtained from high air speeds [47], [48], [49].

4.1.1 The angle control of the blades setting relative to the incoming streams

The blade angle control system in blade turbines allows the blades to be adjusted to current wind conditions. Sensors built into the nacelle are responsible for providing information about the speed and direction of air to the control system. This information is used to generate a control signal in the control system [50], [51], [52]. As a result, the rotor blades are rotated relative to the mounting axis by such an angular value towards the incoming streams or in accordance with them to make the most effective use of their surface and drive purpose.

The same system allows the blades to be positioned so that the aerodynamic drags increase when the wind is too strong. Then the unwanted output power decreases. The increased resistance prevents further increase of the rotor speed. In a situation where the air force is small, the control system reduces aerodynamic drag to increase the rotational speed and maintain a favorable level of work. The biggest advantage of this solution is its speed of action. Perfectly maintains rotor speed in parameters close to maximum efficiency.

4.1.2 Controlled stall

The aircraft engine rotor blades consist of aerodynamic profiles that are selected for the appropriate and specific operating conditions. The blades are shaped from many profiles, just like the air wings. In rotors without the ability to control the blade angle, they are selected on the basis of the calculated average air speeds at which they are to work. It is most often used because it does not require an adjustment system, making the construction simpler. When such a blade is flowing with air of lower or higher speed than expected, the distribution of aerodynamic forces changes along its entire length.

In the design of fixed blades, the thickness of the tip and its twist are taken into account, because at high rotational speed they favor the formation of greater resistance, which causes aerodynamic braking of rotational speed and prevents it from increasing. In addition, the efficiency of electricity generation of this solution is lower due to the inability to adapt to the prevailing conditions.

4.1.3 Basic case

Turbines in an aircraft engine operate at air flow speeds from 5 to 25 m/s. They reach rated power at speeds of around 10 m/s, which is why this value was set in the basic case. The transmission system as well as some parts of the distribution system operate at voltages in the kilovolt range. Therefore, the value 1000 V was set for stator voltages V_{ds} and V_{qs}.

Blade angle β was set to zero in the basic case, which translates into the maximum value of captured power from the air flow. The simulation was carried out in Matlab software for 10 hours. The simulation results are presented in the following charts (Figs. 4-6).

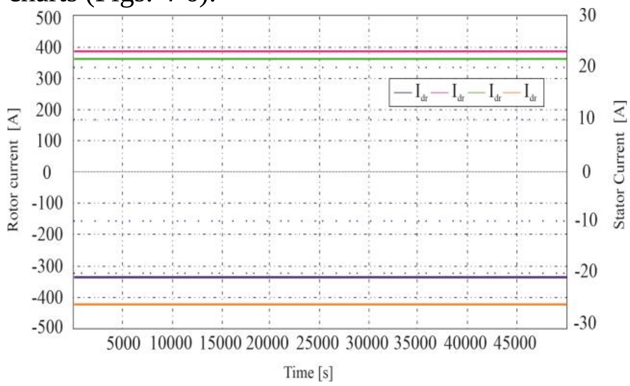

Fig. 4 Graph of current generated over time

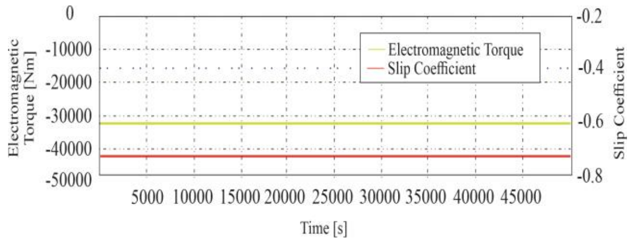

Fig. 5 Graph of resulting torque and slipping over time

As expected, the electromagnetic torque shown in red and the slip shown in navy blue have a negative value.

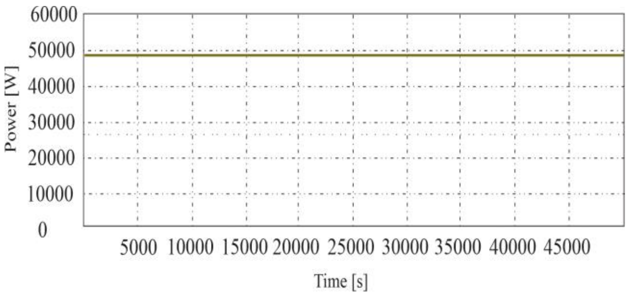

Fig. 6 Graph of turbine power over time

4.1.4 The case of a step change of air velocity

In this case, the effect of increasing air flow velocity from 8 m/s to 10 m/s on the operation of the turbine in a twenty-hour simulation was examined. Initially, the air speed was set to 8 m/s in simulation for 10 hours. After this time, an increase in speed to 10 m/s was set and the work was tested for another 10 hours (Fig. 7).

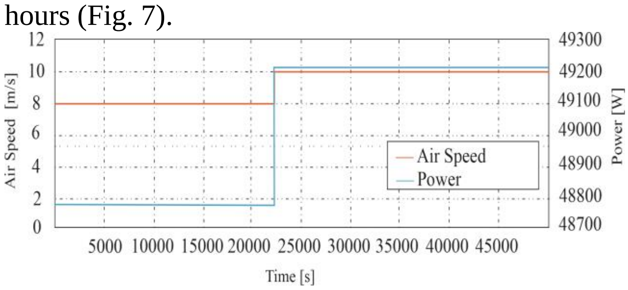

Fig. 7 Graph of the impact of air velocity on output power

An increase in turbine power in the aircraft engine was observed with an increase in air velocity.

4.1.5 The case of a step change in the angle setting of the blades

The turbine response to the set step changes of the blade angle setting is shown in the diagrams (Figs. 8-9).

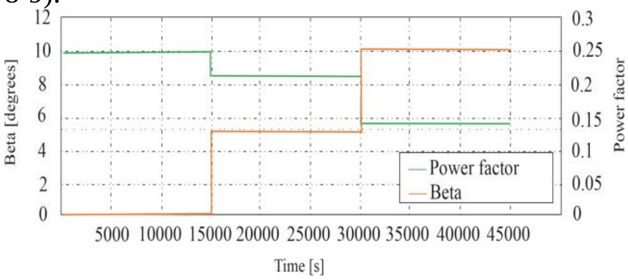

Fig. 8 Graph of the influence of the setting angle β on the C_P turbine power coefficient

The above graph (Fig. 8) shows the impact of changing the setting angle on the turbine power factor. Increasing the angle β (marked in navy blue) directly translates into a decrease in the C_P coefficient (marked in purple).

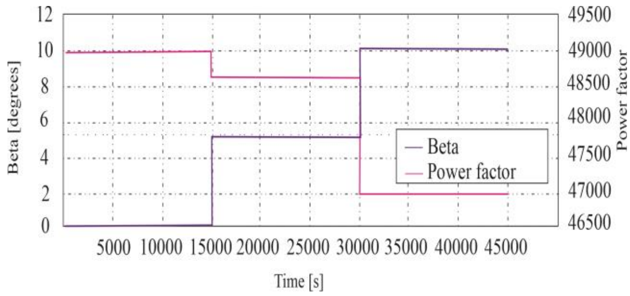

Fig. 9 Graph of the effect of the angle β change on the power P

The graph presented in Fig. 9 shows the situation when by increasing the angle of blades β it is possible to reduce the surplus of generated power, which is unfavorable. This is done by increasing the aerodynamic drag of the blade. The use of this can be found when the air velocity is too high.

5 Conclusions

A model consisting of blades, mechanical parts and an induction current generator was developed to utilize air energy. This model has been implemented for simple simulation of turbine output power in Matlab software. To test the performance and performance of the proposed model, the appropriate conditions were simulated to affect the nature of the operation of the turbine. The model was confronted with a step change in air speed and a change in blade angle setting. Simulated responses of the turbine model with variable working speed, in both cases gave valuable results.

As expected, the power generated increases as the airflow velocity increases, which confirms the need for constant unit control before abnormal operation. A promising way is to control by changing the angle of the blades, because as shown in the simulation, its increase causes a decrease in the air energy used, in the aerodynamic sense. As a result, less output power was obtained. The mentioned model turned out to be computationally efficient, as real dynamic simulation time was introduced.

Conducting many similar tests of supply systems driven by air flow will allow to a large extent exclude the effects of adverse flow. What is more, this method is the basis for the control of these machines, which is why it is recommended to develop it towards maximum efficiency and to look for additional, auxiliary systems to increase work safety. It is desirable to develop such a system that, with its smooth regulation and constant control of parameters, ensures the continuity of electricity supply [53].

References:

[1] E. Levi, Multiphase Electric Machines for Variable Speed Applications, *IEEE Trans. Ind. Electron.*, Vol. 55, No. 5, May 2008, pp. 1893-1909.

[2] Y. Komatsu, Y. Kawabata, M. Kobayashi, T. Kawabata, and E. C. Ejiogu, New Induction Machine Rotor Constants, In: *Proc. ISIE*, , Vol. 2, Jun. 1996, pp. 900-904.

[3] C. I. Hill, S. Bozhko, T. Yang, P. Giangrande, and C. Gerada, More Electric Aircraft Electro-mechanical Actuator Regenerated Power Management, In: *Proc. IEEE Int. Symp. Ind. Electron.*, Jun. 2015, pp. 337-342.

[4] R. Mujal Rosas, O. Boix Aragones, and G. Marin, Three-phase Induction Motor with Spiral Sheet Rotor, In: *Proc. IEEE Int. Symp. Ind. Electron.*, Jun. 2008, pp. 455-460.

[5] D. Platt, Reluctance Motor with Strong Rotor an Isotropy, In: *Conf. Rec. IEEE IAS Annu. Meeting*, Vol. 1, Oct. 1990, pp. 224-229.

[6] J. A. Weimer, The Role of Electric Machines and Drives in the More Electric Aircraft, In: *Proc. IEEE Int. Electr. Mach. Drives Conf. (IEMDC)*, Vol. 1. Jun. 2003, pp. 11-15.

[7] L. Setlak, R. Kowalik, Evaluation of the VSC-HVDC System Performance in Accordance with the More Electric Aircraft Concept, *IEEE Xplore*, 28 June 2018.

[8] V. C. Cavalcanti, and C. R. Andrade, A Trade-off Study of a Bleedless and Conventional Air Conditioning Systems, presented at the *SAE Brasil Congr. Exhib.*, 2008.

[9] R. M. Rosas, O. B. Aragones, and X. C. Fajula, Induction Motor with Spiral sheet rotor, In: *Proc. IEEE Int. Symp. Ind. Electron.*, Jul. 2009, pp. 529-537.

[10] J. W. Lee, H. S. Kim, B. I. Kwon, and B. T. Kim, New Rotor Shape Design for Minimum Torque Ripple of SRM Using FEM, *IEEE Trans. Magn.*, Vol. 40, No. 2, Mar. 2004, pp. 754-757.

[11] D. Gonen, Analysis of a 2-phase Drag-cup Induction Machine, *IEEE Trans. Power App. Syst.*, Vol. PAS-85, No. 1, Jan. 1966, pp. 71-76.

[12] M. Z. Wellingtong, Experimental Investigation of an Induction Motor for High Speed Solid Rotor and Composites, *IEEE Trans. Elect. Mach.*, Vol. 32, No. 6, Jul. 2000, pp. 204-215.

[13] M. R. Krishnamurthy, and V. Veluchamy, Polyphase Induction Machine with Hollow Ferromagnetic Rotor – Part II: Effect of Magnetic Web, *IEEE Trans. Power App. Syst.*, Vol. PAS-91, No. 4, Jul. 1972, pp. 1686-1691.

[14] V. K Mehta, Rohit Mehta, Principles of Electrical Machines, *S Chand, Reprint Edn*., 2006 edition. [6]

[15] L. Setlak, R. Kowalik, Examination of Multi-Pulse Rectifiers of PES Systems Used on Airplanes Compliant with the Concept of Electrified Aircraft, *Applied Sciences (Switzerland)*, Vol. 9, No. 8, 2019/1, E-ISSN:2076-3417.

[16] Jan Melkebeek, Electrical Machines and Drives Fundamentals and Advanced Modelling, *Springer*, 2018. [11]

[17] X. Tu, L.-A. Dessaint, R. Champagne, and K. Al-Haddad, Transient Modeling of Squirrel-cage Induction Machine Considering Air-gap Flux Saturation Harmonics, *IEEE Trans. Ind. Electron*., Vol. 55, No. 7, Jul. 2008, pp. 2798-2809.

[18] A. M. Oliveira, P. Kuo-Peng, N. Sadowski, F. Runcos, R. Carlson, and P. Dular, Finite-element Analysis of a Double-winding Induction Motor with a Special Rotor Bars Topology, *IEEE Trans. Magn.*, Vol. 40, No. 2, Mar. 2004, pp. 770-773.

[19] A. Colin, Turbojet Having an Electricity Generator Arranged in its Fan, U.S. Grant 7 952 244 B2, May 31, 2009.

[20] J. F. Lindsay and T. H. Barton, Parameter Identification for Squirrel-cage Induction Machines, *IEEE Trans. Power App. Syst.*, Vol. PAS-92, No. 1, Jul. 1973, pp. 1287-1291.

[21] M. Apstein and L. M. Blum, Low Inertia Induction Motors, *Trans. Amer. Inst. Elect. Eng.*, Vol. 76, No. 3, Apr. 1957, pp. 253-257.

[22] R. M. Rosas, O. B. Aragones, X. C. Fajula, and A. R. Blanco, Behavior of the Three-phase Induction Motor with Spiral Sheet Rotor, *IEEE Trans. Energy Convers.*, Vol. 24, No. 1, Mar. 2009, pp. 68-76.

[23] R. Glassock, M. Galea, W. Williams, and T. Glesk, Hybrid Electric Aircraft Propulsion Case Study for Skydiving Mission, *Aerospace*, Vol. 4, No. 3, 2017, pp. 1-22.

[24] Y.-H. Chang and P.-C. Shao, Operating Cost Control Strategies for Airlines, *African J. Bus. Manage*, Vol. 5, No. 26, 2011, pp. 10396-103409.

[25] L. Setlak, R. Kowalik, The Effectiveness of On-board Aircraft Power Sources in Line with the Trend of a More Electric Aircraft, *IEEE Xplore*, 28 June 2018.

[26] M. E. Zaim, Non-linear Models for the Design of Solid Rotor Induction Machines, *IEEE Trans. Magn.*, Vol. 35, No. 3, May 1999, pp. 1310-1313.

[27] A. Al-Timimy, P. Giangrande, M. Degano, M. Galea, and C. Gerada, Comparative Study of Permanent Magnet-synchronous and Permanent Magnet-flux Switching Machines for High Torque to Inertia Applications, In: *Proc. IEEE Workshop Elect. Mach. Design, Control Diagnosis*, Apr. 2017, pp. 45-51.

[28] L. Setlak, R. Kowalik, Mathematical Modeling and Simulation of Selected Components On-board Autonomous Power Supply System (ASE), in Accordance with the Concept of a More Electric Aircraft (MEA), *IEEE - Institute of Electrical and Electronics Engineers*, 2017, ISBN: 978-1-5090-6407-6.

[29] T. Feehally, Electro-mechanical Interaction in Gas Turbine-generator Systems for More-Electric Aircraft, Ph.D. Dissertation, Univ. Manchester, Manchester, U.K., 2012.

[30] P. Giangrande, C. I. Hill, S. V. Bozhko, and C. Gerada, A Novel Multi-level Electro-mechanical Actuator Virtual Testing and Analysis Tool, In: *Proc. IET Int. Conf. Power Electron., Mach. Drives*, 2014, pp. 1-6.

[31] K. Vijayakumar, R. Karthikeyan, S. Paramasivam, R. Arumugam, and K. N. Srinivas, Switched Reluctance Motor Modeling, Design, Simulation, and Analysis: A comprehensive review, *IEEE Trans. Magn.*,Vol. 44, No. 12, Dec. 2008, pp. 4605-4617.

[32] C. L. Bowman, Visions of the Future: Hybrid Electric Aircraft Propulsion, *Proc. AIAA Aircraft Electr./Hybrid-Electr. Power Propuls.*, Workshop, Jul. 2016, accessed: Dec. 2017. [Online].Available:https://ntrs.nasa.gov/archive /nasa/casi.ntrs.nasa.gov/20170002633.pdf

[33] S. R. MacMinn and W. D. Jones, A Very High Speed Switched-reluctance Starter-generator for Aircraft Engine Applications, In: *Proc. IEEE Nat. Aerosp. Electron. Conf.*, Vol. 4. May 1989, pp. 1758-1764.

[34] D. V. Makarov, A. S. Khlebnikov, A. V. Geist, and P. A. Bachurin, Generation System with Variable Frequency and Constant amplitude, In: *Proc. 3rd Int. Youth Conf. Energetics (IYCE)*, 2011, pp. 1-9.

[35] C. A. Ferreira, S. R. Jones, W. S. Heglund, and W. D. Jones, Detailed Design of a 30-kW Switched Reluctance Starter/generator System for Agas Turbine Engine Application, *IEEE Trans. Ind. Appl.*, Vol. 31, No. 3, May 1995, pp. 553-561.

[36] F. Cupertino, G. Pellegrino, P. Giangrande, and L. Salvatore, Model Based Design of a Sensorless Control Scheme for Permanent Magnet Motors Using Signal Injection, In: *Proc. Energy Convers. Congr. Expo.*, Atlanta, GA, USA, Sep. 2010, pp. 3139-3146.

[37] A.V. Radun, C.A. Ferreira, and E. Richter, Two Channel Switched Reluctance Starter/generator Results, In: *Proc. Appl. Power Electron. Conf. (APEC)*, Vol. 1, Feb. 1997, pp. 546-552.

[38] M. Hirst, A. Mcloughlin, P. J. Norman, and S. J. Galloway, Demonstrating the More Electric Engine: A Step Towards the Power Optimised Aircraft, *IET Electr. Power Appl.*, Vol. 5, No. 1, 2011, pp. 3-13.

[39] P. Giangrande, F. Cupertino, and G. Pellegrino, Modelling of Linear Motor and Effects for Saliency Based Sensorless Control, In: *Proc. IEEE Energy Convers. Congr. Expo*., Atlanta, GA, USA, Sep. 2010, pp. 3261-3268.

[40] A. Al-Timimy et al., Design and Optimization of a High Power Density Machine for Flooded Industrial Pump, In: *Proc. Int. Conf. Elect. Mach.*, Lausanne, Switzerland, 2016, pp. 1480-1486.

[41] Aircraft Commerce; Can the 787 & A350 Transform the Economicsof Long-Haul Services? Aircraft Commerce, *Nimrod Publications*, Horsham, U.K., Feb./Mar. 2005.

[42] J. Brombach, A. Lücken, B. Nya, M. Johannsen, and D. Schulz, Comparison of Different Electrical HVDC-Architectures for Aircraft Application, In: *Proc. Elect. Syst. Aircraft, Railway Ship Propuls.*, 2012, pp. 1-6.

[43] L. Setlak, R. Kowalik, Modern Technological Solutions in Generation, Transmission and Distribution of Electricity in 'Conventional' vs. 'More Electric' Aircrafts, *IEEE - Institute of Electrical and Electronics Engineers*, ISBN: 978-1-5386-1529-4, 2017.

[44] M. Hepperle, Electric Flight - Potential and Limitations, In: *Proc. Energy Efficient Technol. Concepts Operation Conference*, Lisbon, Portugal: NATO Science Technology Organization, October 2012. [Online]. Available: http://elib.dlr.de/78726/

[45] J. Brombach, T. Schröter, A. Lücken, and D. Schulz, Optimized Cabin Power Supply with a ±270 V DC Grid on a Modern Aircraft, In: *Proc. 7th Int. Conf.-Workshop Compat. Power Electron. (CPE)*, 2011, pp. 425-428.

[46] I. Moir and A. G. Seabridge, Vehicle Management Systems in Military Avionics Systems, New York, NY, USA, *Wiley*, 2006, pp. 399-401.

[47] L. Setlak, R. Kowalik, Mathematical Model and Simulation of Selected Components of the EPS of the Aircraft, Providing the Operation of

On-board Electrical Equipment and Systems in Accordance with MEA/AEA Concept, *IEEE - Institute of Electrical and Electronics Engineers*, ISBN: 978-1-5386-1529-4, 2017.

[48] Boeing. Current Market Outlook 2017–2036, Accessed: Dec. 2017. [Online].Available: http://www.boeing.com/commercial/market/current-market-outlook-2017/[85]

[49] Airbus. Airbus, Rolls-Royce, and Siemens Team up for Electric Future. Accessed: December 2017. [Online]. Available: http://www.airbus.com/newsroom/press-releases/en/2017/11/airbus–rolls-royce–and-siemens-team-up-for-electric-future-par.html

[50] J. Hale. 787 Design for Maintainability, ATEC, Accessed: Dec. 2017. [Online]. Available: http://www.vaughn.edu/assets/downloads/ATEC-2008-01.pdf

[51] Reported Operating Cost and Utilization of More Than 500 Wide-Body Aircraft. Accessed: Dec. 2017. [Online]. Available: http://www.planestats.com/bhsw_2014sep

[52] M. E. Elbuluk and M. D. Kankam, Potential Starter/generator Technologies for Future Aerospace Applications, *IEEE Aerosp. Electron. Syst. Mag.*, Vol. 12, No. 5, May 1997, pp. 24-31.

[53] D. A. Torrey, Switched Reluctance Generators and Their Control, *IEEE Trans. Ind. Electron.*, Vol. 49, No. 1, Feb. 2002, pp. 3-14.